

1 Perforin-2 limits pathogen proliferation at the maternal-fetal interface

2

3 *Petoria Gayle**, *Vanessa McGaughey**, *Rosmely Hernandez**, *Marina Wylie*†*, *Rachel C.*

4 *Colletti*†*, *Ka Lam Nguyen*†*, *Marshall Arons**, *Laura Padula**, *Natasa Strbo**, *Kurt Schesser**

5

6 *Department of Microbiology & Immunology, University of Miami Miller School of Medicine,

7 Miami, FL, USA

8

9 Corresponding Author: Kurt Schesser, Department of Microbiology and Immunology, University
10 of Miami Miller School of Medicine, 1600 NW 10th Avenue, Miami, FL 33136.

11 kschesser@med.miami.edu

12

13 † Current addresses: Uniformed Services University of the Health Sciences, Bethesda, MD (MW);
14 Philadelphia College of Osteopathic Medicine, Philadelphia, PA (RCC); The University of Illinois
15 at Urbana-Champaign, Champaign, IL (KLN).

16

17 PG and KS conceived the project, designed the experiments, and interpreted the data. All
18 experiments and data collection were performed by PG with assistance by VM, RH, MW, RCC,
19 KLN, MA, and KS. Contributions to the development of methodologies were made by LP and NS.

20 The manuscript was primarily written by PG with assistance by KS.

21 *Abstract:*

22 Placental immune responses are highly regulated to strike a balance between protection and
23 tolerance. For relatively mild infections, protection encompasses both the mother and fetus;
24 however, during worsening conditions, protection becomes exclusively reserved for the mother.
25 Previously, we and others have shown that the host factor Perforin-2 plays a central role in
26 protecting mice and cells against infection. Here, we analyzed Perforin-2 activity in the mouse
27 placenta to determine whether Perforin-2 plays a similarly protective role. We show that Perforin-
28 2 is critical for inhibiting *Listeria monocytogenes* colonization of the placenta and fetus and that
29 this protection is due to both maternal and fetal-encoded Perforin-2. *Perforin-2* mRNA is readily
30 detectable in individual immune cells of the decidua and these levels are further enhanced
31 specifically in decidual macrophages during high-dose infections that result in fetal expulsion.
32 Unexpectedly, inductive Perforin-2 expression in decidual macrophages did not occur during
33 milder infections in which fetal viability remained intact. This pattern of expression significantly
34 differed from that observed in splenic macrophages in which inductive Perforin-2 expression was
35 observed in both high and mild infection conditions. In the placenta, inductive Perforin-2
36 expression in decidual macrophages was co-incident with their polarization from a M2 to M1
37 phenotype that normally occurs in the placenta during high-burden infections. Our results suggest
38 that Perforin-2 is part of a host response that is protective either for both the mother and fetus in
39 milder infections or exclusively for the mother during high-dose infections.

40 *Introduction:*

41 The balance between host defense and tolerance during pregnancy is achieved both by the
42 modulation of the maternal immune system towards the semi-allogenic fetus as well as through
43 the barrier function of the placenta. Despite these safeguards, infections contribute approximately
44 25% of stillbirths in the United States, largely due to the ability of specific pathogens, including
45 *Listeria monocytogenes*, to colonize the placenta (McClure et al. 2010). *L. monocytogenes* is
46 widely used in hematogenous infection models to study host-pathogen interactions in the placenta
47 (Lamond and Freitag 2018). While these models have advanced our understanding of the
48 pathogenesis of placental infections, there still remains the need to further understand the
49 mechanisms of immune defense in coordination with fetal tolerance during placental infection.

50 Numerous studies have shown that infections during pregnancy can disrupt the highly
51 controlled inflammatory response and result in pregnancy complications such as miscarriages or
52 spontaneous abortion (Kim et al. 2005; Mor et al. 2017; Rodrigues-Duarte et al. 2018). These
53 pregnancy related complications are commonly attributed to the activation of the innate immune
54 response. Specifically, macrophages of the decidua, the maternal component of the placenta, have
55 been shown to be highly dynamic during pregnancy. These cells change and respond to the
56 inflammatory environment of the placenta expressing characteristics of the classically activated
57 phenotype, M1, in early and late pregnancy and resembling the M2 phenotype during the mid-
58 stage of pregnancy (Shapouri-Moghaddam et al. 2018; Zhang et al. 2017). Excessive levels of pro-
59 inflammatory M1 macrophages have been linked to abnormal pregnancy outcomes including pre-
60 term labor and fetal mortality (Jena et al. 2019; Svensson-Arvelund and Ernerudh 2015; Wang et
61 al. 2011; Xu et al. 2016). It has also been shown that *L. monocytogenes* can trigger M1 polarization
62 in the placenta (Benoit et al. 2008). Studying the role of innate immune factors within the placenta

63 is important to enhance our understanding of how to prevent the devastating effects of infection
64 during pregnancy.

65 In vertebrates there are three pore-forming factors that protect against microbial pathogens.
66 Complement component 9 (C9) and Perforin-1 possess membrane-attack-complex-perforin
67 (MACPF) domains that mediate their polymerization and pore formation. The third and most
68 recently identified vertebrate MACPF-containing factor, Perforin-2, is found in the earliest
69 evolved animals, and is ancestral to C9 and Perforin-1 (D'Angelo et al. 2012). Unlike the
70 Complement Factors and Perforin-1 that are secreted from cells, Perforin-2 is an integral
71 membrane protein. In human and mouse cells *Perforin-2* mRNA is constitutively present in
72 macrophages and is induced in fibroblastic cells following infection or exposure to inflammatory
73 signals (McCormack et al. 2013). Perforin-2 plays a major role in protecting mice from *Listeria*,
74 *Salmonella*, *Staphylococcus*, and *Yersinia* infections (McCormack et al. 2015a; 2015b; 2016). *In*
75 *vitro*, Perforin-2 restricts intracellular *L. monocytogenes* proliferation by a pH-dependent
76 mechanism in both primary peritoneal macrophages and fibroblastic cells suggesting that the rapid
77 development of listeriosis in *Perforin-2* *-/-* mice is due to defects in cellular killing activity
78 (McCormack et al. 2016). Recently it has been shown that Perforin-2 directly impacts type I
79 interferon signaling by physically interacting with the IFN- α and $-\beta$ receptors 1 and 2 (McCormack
80 et al. 2020). Whether the bactericidal activity of Perforin-2 involves the interferon signaling
81 machinery remains to be determined.

82 Here we tested whether Perforin-2 plays a protective role in limiting colonization of *L.*
83 *monocytogenes* in the mouse placenta. Additionally, we analyzed *Perforin-2* mRNA expression in
84 individual cells of the placenta following infection to determine whether *Perforin-2* expression
85 levels change during infection.

86 *Materials and Methods:*

87 *Mice, microbes, and infections*

88 Wild-type BALB/c and C57BL/6 *Perforin-2* ^{+/+} and *Perforin-2* ^{-/-} littermates (McCormack et al.
89 2015a) were bred in the animal care facility at the University of Miami Miller School of Medicine,
90 Miami, FL. All animal procedures were approved by the Institutional Animal Care and Use
91 Committee, University of Miami Miller School of Medicine (protocol 19-075). Animals were
92 housed under a circadian cycle (12hr light/12hr dark cycle). Virgin female mice were mated
93 between 6 - 12 weeks of age, and checked daily for estrous stage and copulatory plugs. Presence
94 of a plug was denoted as gestation day (GD) 0.5. Weight gain was monitored on GD 4.5 through
95 GD 12.5 to confirm pregnancy. *L. monocytogenes* (10403S) were grown in brain heart infusion
96 media at 37 °C with vigorous shaking to mid-log phase. Mice at GD 12.5 were infected
97 intravenously with doses as indicated in figure legends. At 44 hours post infection (hpi), mice were
98 humanely euthanized and uterine horns, livers, and spleens were removed and processed for either
99 single cell analysis (see below) or colony forming unit (CFU) assays. For CFU assays, placentas
100 (including decidual tissue), fetuses, and livers were further dissected and homogenized using a fine
101 wire mesh to grind the tissues in sterile water containing 0.05% Tween. The resulting tissue
102 homogenates were diluted and plated on Luria Broth agar to determine *L. monocytogenes* titers. In
103 the experiments using heterogenic matings, fetal tissue homogenates were used for genotyping.

104 *Preparation of single-cell suspensions*

105 Following their removal, uterine horns were dissected to remove individual fetal-placental units
106 (FPU), each FPU was further dissected to isolate decidual tissue. Livers (minced) and pooled
107 deciduae were incubated in 2 mg/mL collagenase D (Roche) at 37 °C for 30 – 40 minutes with
108 agitation. The resulting cell suspensions were then washed with cold IMDM (Life Technologies)

109 + 10% heat-inactivated FBS (Sigma-Aldrich), passed through a 70 μ m filter followed by passaging
110 through a 40 μ m filter (VWR International, Radnor, PA). Spleens were gently homogenized
111 through 70 μ m filters and similarly washed and passed through 40 μ m filters. The resulting single
112 cells were then centrifuged at 500g for 5 min at 4°C, treated with ACK Lysing Buffer (Life
113 Technologies Corporation) for 5 minutes to remove red blood cells, and finally washed with
114 IMDM + 10% FBS. Total viable cells were determined using the Vi-Cell XR Cell Viability
115 Analyzer (Beckman Coulter).

116 *Single cell analysis*

117 Isolated cells were washed in FACS staining buffer and incubated with anti-CD16/32 (clone
118 2.4G2) to block FcRs for 10 mins followed by an incubation with Live/Dead fixable yellow dead
119 cell stain (ThermoFisher) and fluorescent-conjugated monoclonal antibodies (mAbs) for 30 min.
120 The following anti-mouse mAbs were used for analysis: CD45 (30-F11; BioLegend), CD3 (17A2;
121 BioLegend), F4/80 (BM8; BioLegend), CD11b (M1/70; BioLegend), Ly6C (HK1.4; BioLegend),
122 Ly6G (1A8; BioLegend), CD335 (29A1.4; BioLegend), MHC II (M5/114.15.2; BD Biosciences),
123 CD206 (C068C2; BioLegend). Depending on the experiment, samples were either immediately
124 analyzed by flow cytometry using a Sony SP6800 Spectral Analyzer or further processed to
125 determine *Perforin-2* mRNA levels. Branched oligonucleotide signal amplification was used to
126 determine *Perforin-2* mRNA levels in individual cells (PrimeFlow; ThermoFisher Scientific).
127 Briefly, single cell suspensions were stained for surface antigens as described above, then fixed,
128 permeabilized, and incubated with probes specific for *Perforin-2* transcripts (Assay Id: VB1-
129 20172-PF; ThermoFisher Scientific). Cells were then subjected to a series of signal amplification
130 cycles and then analyzed by flow cytometry as described above using FlowJo software (BD
131 Biosciences).

132 *Results:*

133 *Perforin-2 limits pathogen colonization at the maternal-fetal interface*

134 Pregnant wild-type and isogenic Perforin-2-deficient (*Perforin-2* *-/-*) mice were infected
135 intravenously on gestation day (GD) 12.5 (i.e., mid-gestation) with *L. monocytogenes*. At 44 hours
136 post infection, dams were humanely euthanized and livers and fetal placental units (FPU) were
137 evaluated for *L. monocytogenes* by colony forming unit (CFU) assay. In infected *Perforin-2* *+/+*
138 dams, 54% (12/22) of the placentas and 14% (3/22) of fetuses possessed detectable levels of *L.*
139 *monocytogenes* (**Fig. 1**). Dosages that result in approximately 50% of placentas in *Perforin-2* *+/+*
140 mice becoming infected will henceforth be referred to as placental dose 50 (PD₅₀). In contrast,
141 *Perforin-2* *-/-* mice harboring comparable levels of *L. monocytogenes* in the liver as *Perforin-2*
142 *+/+* dams, 88% (15/17) of the placentas and 71% (12/17) of fetuses possessed detectable levels of
143 *L. monocytogenes*. These results suggest that Perforin-2 may play a significant role in limiting *L.*
144 *monocytogenes* colonization of the placenta and fetus.

145

146 *Maternal and fetal-derived Perforin-2 contributes to protection against infection in the placenta*

147 The placenta is a chimeric organ that consists of maternally-derived tissue and fetal-derived
148 trophoblast cells. A heterogenic mating strategy was used to evaluate the specific contributions of
149 maternal- and fetal-derived Perforin-2 in limiting *L. monocytogenes* colonization in the placenta.
150 Initially, *Perforin-2* *-/-* female mice were crossed to *Perforin-2* *+/-* males (generating
151 approximately 50% *Perforin-2* *+/-* and 50% *Perforin-2* *-/-* fetuses) and at GD 12.5, dams were
152 infected with PD₅₀ *L. monocytogenes* and analyzed as described above. A representative dam is
153 shown in which the infection burdens of FPUs containing *Perforin-2* *+/-* fetuses are generally
154 lower than FPUs containing *Perforin-2* *-/-* fetuses (**Fig. 2A**). In compiled data from 5 dams, the

155 placentas associated with *Perforin-2* +/- fetuses (designated as T(+/-)) had significantly lower
156 infection burdens compared to placentas associated with *Perforin-2* -/- fetuses (designated as T(-
157 -/-)). A similar reduction in infection burden was observed in *Perforin-2* +/- fetuses compared to
158 *Perforin-2* -/- fetuses (**Fig. 2B**) indicating that fetal-derived Perforin-2 protects the placenta from
159 infection. In reciprocal matings, in which *Perforin-2* +/- female mice were crossed with *Perforin-*
160 *2* -/- males and infected at GD 12.5, a more modest protective effect of fetal-derived Perforin-2
161 was observed (**Fig. 2C**), possibly indicating that maternal-derived Perforin-2 partially masks the
162 protective effect of fetal-derived Perforin-2. Collectively these data show that both maternal- and
163 fetal-derived Perforin-2 contribute to protecting the placenta from being colonized by a bloodborne
164 pathogen.

165

166 *Perforin-2* expression is induced in placental immune cells following infection

167 The maternal component of the placenta, the decidua, is the initial colonization site of various
168 bloodborne pathogens including *L. monocytogenes* (Rizzuto et al. 2017). We initially analyzed the
169 cellular composition of the decidua and the liver in uninfected and infected mid-gestation mice.
170 Previously we and others showed that the immune cell composition in the liver in non-pregnant
171 mice undergoes substantial changes following *L. monocytogenes* infection (Gregory et al. 2002;
172 Blériot et al. 2015; Gayle et al. 2019). There was a similar pattern of changes in the liver observed
173 in mid-gestation pregnant mice following infection, including a marked disappearance of resident
174 macrophages (CD11b^{lo}/F4/80⁺) and the infiltration of inflammatory monocytes and neutrophils
175 (CD11b⁺/F4/80⁻) (**Fig. 3A**). In contrast, in the decidua of the same mice, there were no significant
176 changes in the resident macrophages (CD11b⁺/F4/80⁺) or other cell types following infection (**Fig.**
177 **3B**). From GD 12.5 – 14.5 pregnant mice approximately a million cells are typically isolated from

178 individual decidua of which ~20% are CD45⁺. The 4 x 10⁵ CD45⁺ cells per decidua is composed
179 of approximately 20% CD11b⁻/F480⁻ (primarily NK cells), 30% CD11b⁺/F480⁻ (monocytes and
180 neutrophils), and 40% CD11b⁺/F480⁺ (macrophages).

181 *Perforin-2* mRNA levels were assayed in individual decidual cells to determine both cell
182 type-specific expression and whether expression levels change following infection. To ensure that
183 all placentas within each pregnant mouse became colonized by *L. monocytogenes* during the 44 hr
184 infection period, the doses used for these experiments will be referred to as placental dose 100%
185 (PD₁₀₀) that are 2- to 4-fold higher than the 'low-dose' experiments shown in Figs. 1 and 2. As
186 described earlier, pregnant mice (GD 12.5) were either left uninfected or infected with *L.*
187 *monocytogenes* and following 44 hours of infection, FPU were collected and placentas were
188 further dissected to isolate decidual cells. Pooled decidual cells from each individual dam were
189 analyzed for cell surface markers and *Perforin-2* mRNA levels. In uninfected dams, *Perforin-2*
190 mRNA was readily detected in CD45⁺ decidual cells and this signal was enhanced 2- to 3-fold in
191 CD45⁺ decidual cells isolated from infected dams (**Fig. 4A, B**). A similar 2- to 3-fold infection-
192 dependent increase in *Perforin-2* mRNA levels was also observed in CD45⁺ splenic cells derived
193 from the same mice (**Fig. 4C**).

194 Of the three major CD45⁺ subsets found in the GD 12.5 decidua of BALB/c mice (see **Fig.**
195 **3B**), infection-induced enhancement of *Perforin-2* mRNA levels occurred primarily in the
196 CD11b⁺F4/80⁺ macrophages (**Fig. 5A,B**). This infection-induced increase also occurred in the
197 CD45⁺ splenic macrophages derived from the same mouse (**Fig. 5C**). In addition, *Perforin-2*
198 mRNA was also specifically induced in infected decidual and splenic CD11b⁺F4/80⁺ macrophages
199 isolated from C57BL/6 mice (**Fig. 5D-F**). These data show that *Perforin-2* mRNA levels increase
200 in immune cells of the decidua following infection and that this increase primarily occurs in

201 macrophages.

202

203 *Reduced infection dosages result in modest changes in Perforin-2 mRNA levels in decidual*
204 *macrophages*

205 As noted earlier, the *Perforin-2* expression experiments shown in Figs. 4 and 5 used infective doses
206 (PD₁₀₀) that resulted in all placentas becoming colonized with *L. monocytogenes* by 44 hpi.
207 Unexpectedly, when these experiments were performed with 2- to 4-fold lower doses of *L.*
208 *monocytogenes* in which approximately 50% of placentas had become colonized by *L.*
209 *monocytogenes* by 44 hpi (PD₅₀), there was little to no difference in *Perforin-2* mRNA levels
210 between decidual macrophages isolated from uninfected and infected GD 12.5 pregnant mice (**Fig.**
211 **6A,B**). In contrast, in the same mice *Perforin-2* mRNA levels were significantly elevated in splenic
212 macrophages isolated from infected mice compared to uninfected mice (**Fig. 6C**). A similar pattern
213 of *Perforin-2* expression in decidual and splenic macrophages was observed in pregnant GD 12.5
214 C57BL/6 mice infected at PD₅₀ (**Fig. 6D,E**). These findings suggest that in the placenta there is a
215 bacterial dose-dependent induction of *Perforin-2* mRNA.

216

217 *Perforin-2 mRNA levels are elevated in M1 decidual macrophages*

218 In humans and mice, decidual macrophages at mid-gestation are primarily of the M2 phenotype
219 and polarization of these macrophages to the inflammatory M1 phenotype is associated with a
220 variety of complications that can lead to premature pregnancy termination (Brown et al. 2014; Jena
221 et al. 2019; Svensson-Arvelund and Ernerudh 2015; Xu et al. 2016). To determine the infection-
222 specific phenotype of decidual macrophages in our model, pregnant GD 12.5 mice were either left
223 uninfected or infected with *L. monocytogenes* at PD₁₀₀. Following their isolation, decidual cells

224 were stained for M1 and M2 specific markers and analyzed by flow cytometry. Macrophages were
225 defined as single, live, CD45⁺, CD11b⁺, F4/80⁺, Ly6C^{lo}, and Ly6G⁻ cells (**Fig. 7A**). Macrophages
226 were then further classified as either M1 (CD206⁻ MHCII^{hi}) or M2 (CD206⁺ MHCII^{lo}) in
227 uninfected and infected dams. Consistent with previously published findings cited above, decidual
228 macrophages isolated from uninfected dams were primarily M2. In contrast, decidual macrophages
229 isolated from infected dams contained lower frequencies of CD206⁺ cells and higher frequency of
230 MHCII cells indicative of a M1-skewed phenotype (**Fig. 7**). When GD 12.5 mice were infected
231 with a reduced dose (PD₅₀) of *L. monocytogenes*, the M1/M2 distribution of decidual macrophages
232 at 44 hpi did not appreciatively differ from that observed in decidual macrophages isolated from
233 uninfected GD 12.5 mice (*not shown*).

234 Decidual macrophages isolated from uninfected dams at mid-term pregnancy (GD 12.5)
235 were stained for M1 and M2 specific markers as described above and subsequently analyzed for
236 *Perforin-2* mRNA levels. In every pregnant mouse examined, *Perforin-2* mRNA levels were
237 notably elevated in M1 decidual macrophages compared to M2 decidual macrophages (**Fig. 8**).
238 Collectively, these data show that at high pathogen burdens M1 macrophages with heightened
239 *Perforin-2* mRNA levels predominate in the placenta.

240 *Discussion:*

241 A unique challenge in both the operation as well as the study of immune responses
242 occurring during pregnancy is that protection for the host may not always encompass the fetus.
243 While the placenta acts as an immunological and physical barrier for fetal protection, it is
244 susceptible to pathogens capable of colonizing this tissue and, under worsening conditions, can
245 reorient towards an exclusively maternal protective response (Robbins and Bakardjiev 2012;
246 Zeldovich and Bakardjiev 2012; Bonney and Johnson 2019; Jena et al. 2019). Decidual
247 macrophages have been shown to be critical for the plasticity of the placental response in being
248 important for both the maintenance of fetal tolerance as well as responding to inflammatory and/or
249 infectious conditions that can result in immune activation against the fetus (Brown et al. 2014;
250 Wang et al. 2018).

251 We show here that Perforin-2 plays a significant role during *L. monocytogenes* infection in
252 the placenta and fetus. We additionally found that fetal-derived Perforin-2 in the placenta
253 contributes to limiting *L. monocytogenes* infection, although there is a dominance in regards to the
254 maternal expression of Perforin-2. These findings are consistent with published data showing that
255 the maternal-derived decidua is the initial site of infection and the first line of defense in
256 bloodborne *L. monocytogenes* infections (Rizzuto et al. 2017). In analysis of *Perforin-2* mRNA
257 levels in individual decidual cells, we found that CD45⁺ cells possessed abundant transcripts, and
258 specific to decidual macrophages, these levels became elevated in infections with high pathogen
259 loads. This inductive *Perforin-2* expression in decidual macrophages correlated with their
260 polarization from the tolerogenic M2 phenotype to the inflammatory M1 phenotype. In these
261 experiments with high pathogen loads (i.e., PD₁₀₀; 5 – 10 x 10⁵ CFU), dams often displayed typical
262 signs of listeriosis at 44 hpi including ruffled fur, hunched backs, and slowed movement. Also

263 there would occasionally be FPU observed in the cage housing presenting with darkened uterine
264 horns and loss of fetal structures in remaining fetuses, all indicative of maternal immune activation
265 (MIA) (Goldstein et al. 2017). In contrast, there was little to no inductive *Perforin-2* expression in
266 decidual macrophages in infections with relatively lower pathogen loads (i.e., PD₅₀; 2 x 10⁵ CFU)
267 in which neither disease symptoms nor fetal expulsions occur. These findings indicate that
268 inductive *Perforin-2* expression in deciduae is associated with a pathological shift in macrophage
269 phenotype.

270 In understanding *Perforin-2* expression in decidual macrophages, it is worth noting that
271 there are three immunological stages of pregnancy (Mor et al. 2017). At the early stage of
272 pregnancy, when the blastocyst is implanted into the uterine wall, there is increased inflammation
273 and a Th₁-biased environment, during which there is a predominance of M1 macrophages in the
274 decidua. It has been shown that this inflammation is not in response to the invading fetal antigens
275 but that there is an active recruitment by the trophoblast cells in an effort to educate immune cells
276 towards fetal tolerance. The mid-stage of pregnancy is a period of fetal growth and when fetal
277 tolerance is the most important, as pathological conditions that lead to MIA can result in a breach
278 of fetal tolerance and therefore fetal rejection (Mor et al. 2017). In line with this, the mid-term of
279 pregnancy represents an anti-inflammatory state, generating a tolerogenic Th₂-type immune
280 environment in which M2 macrophages dominate within deciduae. Lastly, the late stage of
281 pregnancy again requires inflammation that is necessary for labor induction and is characterized
282 by a Th₁ immune response in which again there is a predominance of M1 macrophages.

283 Pathogens capable of crossing the placental barrier can take advantage of the anti-
284 inflammatory microenvironment of the placenta during the mid-stage of pregnancy. However,
285 once a certain threshold is reached and MIA occurs, fetal tolerance can be disrupted and result in

286 pregnancy termination (Bonney and Johnson 2019). Perforin-2 serves both a protective function
287 in sub-MIA infections (i.e., as shown in the PD₅₀ experiments [Figs. 1 and 2]) as well as becoming
288 elevated during infections in which MIA is triggered (Fig. 5). Collectively, our investigation may
289 indicate that Perforin-2 is a component that acts to protect either both the mother and fetus (sub-
290 MIA infections) or exclusively the mother (MIA infections).

291 *References:*

292 Benoit M, Desnues B, Mege JL. Macrophage polarization in bacterial infections. *J Immunol.*
293 2008 Sep 15;181(6):3733-9.

294

295 Blériot C, Dupuis T, Jouvion G, Eberl G, Disson O, Lecuit M. Liver-
296 resident macrophage necroptosis orchestrates type 1 microbicidal inflammation and type-2-
297 mediated tissue repair during bacterial infection. *Immunity.* 2015 Jan 20;42(1):145-58

298

299 Bonney EA, Johnson MR. The role of maternal T cell and macrophage activation in preterm
300 birth: Cause or consequence? *Placenta.* 2019 Apr;79:53-61.

301

302 Brown MB, von Chamier M, Allam AB, Reyes L. M1/M2 macrophage polarity in normal and
303 complicated pregnancy. *Front Immunol.* 2014 Nov 24;5:606.

304

305 Gayle P, Freitag NE, Strbo N, Schesser K. Using a Bacterial Pathogen to Probe for Cellular and
306 Organismic-level Host Responses. *J Vis Exp.* 2019 Feb 22;(144).

307

308 Goldstein JA, Norris SA, Aronoff DM. DOHaD at the intersection of maternal immune
309 activation and maternal metabolic stress: a scoping review. *J Dev Orig Health Dis.* 2017
310 Jun;8(3):273-283.

311

312 Gregory SH, Cousens LP, van Rooijen N, Döpp EA, Carlos TM, Wing EJ. Complementary
313 adhesion molecules promote neutrophil-Kupffer cell interaction and the elimination of bacteria
314 taken up by the liver. *J Immunol.* 2002 Jan 1;168(1):308-15.

315

316 Jena MK, Nayak N, Chen K, Nayak NR.

317 Role of Macrophages in Pregnancy and Related Complications.

318 *Arch Immunol Ther Exp (Warsz).* 2019 Oct;67(5):295-309.

319

320 Kim S, Lee DS, Watanabe K, Furuoka H, Suzuki H, Watarai M. Interferon-
321 gamma promotes abortion due to Brucella infection in pregnant mice. BMC Microbiol. 2005
322 May 4;5:22.
323
324 Lamond NM, Freitag NE. Vertical Transmission of *Listeria monocytogenes*: Probing the Balance
325 between Protection from Pathogens and Fetal Tolerance. Pathogens. 2018 May 25;7(2).
326
327 Rizzuto G, Tagliani E, Manandhar P, Erlebacher A, Bakardjiev AI. Limited Colonization
328 Undermined by Inadequate Early Immune Responses Defines the Dynamics of Decidual
329 Listeriosis. Infect Immun. 2017 Jul 19;85(8).
330
331 Li W, Chang Y, Liang S, Zhong Z, Li X, Wen J, Zhang Y, Zhang J, Wang L, Lin H, Cao X,
332 Huang H, Zhong F. NLRP3 inflammasome activation contributes to *Listeria monocytogenes*-
333 induced animal pregnancy failure. BMC Vet Res. 2016 Feb 24;12:36.
334
335 McClure EM, Dudley DJ, Reddy UM, Goldenberg RL. Infectious causes of stillbirth:
336 a clinical perspective. Clin Obstet Gynecol. 2010 Sep;53(3):635-45.
337
338 McCormack R, and Eckhard R. Podack. 2015. "Perforin-2/Mpeg1 and Other Pore-Forming
339 Proteins throughout Evolution." *Journal of Leukocyte Biology* 98(5):761–68.
340
341 McCormack R, Bahnan W, Shrestha N, Boucher J, Barreto M, Barrera CM, Dauer EA, Freitag
342 NE, Khan WN, Podack ER, Schesser K. Perforin-2 Protects Host Cells and Mice by Restricting
343 the Vacuole to Cytosol Transitioning of a Bacterial Pathogen. Infect Immun. 2016 Mar
344 24;84(4):1083-1091.
345
346 McCormack R, de Armas LR, Shiratsuchi M, Ramos JE, Podack ER. Inhibition of intracellular
347 bacterial replication in fibroblasts is dependent on the perforin-like protein (perforin-2) encoded
348 by macrophage-expressed gene 1. J Innate Immun. 2013;5(2):185-94.
349

350 McCormack RM, de Armas LR, Shiratsuchi M, Fiorentino DG, Olsson ML, Lichtenheld MG,
351 Morales A, Lyapichev K, Gonzalez LE, Strbo N, Sukumar N, Stojadinovic O, Plano GV,
352 Munson GP, Tomic-Canic M, Kirsner RS, Russell DG, Podack ER. Perforin-2 is essential for
353 intracellular defense of parenchymal cells and phagocytes against pathogenic bacteria. *Elife*.
354 2015 Sep 24;4. pii: e06508.
355
356 McCormack R, Hunte R, Podack ER, Plano GV, Shembade N. An Essential Role for Perforin-2
357 in Type I IFN Signaling. *J Immunol*. 2020 Apr 15;204(8):2242-2256
358
359 Money KM, Barke TL, Serezani A, Gannon M, Garbett KA, Aronoff DM, Mirnics K.
360 Gestational diabetes exacerbates maternal immune activation effects in the developing brain.
361 *Mol Psychiatry*. 2018 Sep;23(9):1920-1928.
362
363 Mor G, Aldo P, Alvero AB. The unique immunological and microbial aspects of pregnancy. *Nat*
364 *Rev Immunol*. 2017 Aug;17(8):469-482.
365
366 Rizzuto G, Tagliani E, Manandhar P, Erlebacher A, Bakardjiev AI.
367 Limited Colonization Undermined by Inadequate Early Immune Responses Defines the Dynamic
368 s of Decidual Listeriosis. *Infect Immun*. 2017 Jul 19;85(8).
369
370 Robbins JR, Bakardjiev AI. Pathogens and the placental fortress. *Curr Opin Microbiol*. 2012
371 Feb;15(1):36-43.
372
373 Rodrigues-Duarte L, Pandya Y, Neres R, Penha-Gonçalves C. Fetal and Maternal Innate
374 Immunity Receptors Have Opposing Effects on the Severity of Experimental Malaria in
375 Pregnancy: Beneficial Roles for Fetus-Derived Toll-Like Receptor 4 and Type I Interferon
376 Receptor 1. *Infect Immun*. 2018 Apr 23;86(5).
377
378 Shapouri-Moghaddam A, Mohammadian S, Vazini H, Taghadosi M, Esmaili SA, Mardani F,
379 Seifi B, Mohammadi A, Afshari JT, Sahebkar A. Macrophage plasticity, polarization,
380 and function in health and disease. *J Cell Physiol*. 2018 Sep;233(9):6425-6440

381
382 Strbo N, Pastar I, Romero L, Chen V, Vujanac M, Sawaya AP, Jozic I, Ferreira ADF, Wong LL,
383 Head C, Stojadinovic O, Garcia D, O'Neill K, Drakulich S, Taller S, Kirsner RS, Tomic-Canic
384 M. Single cell analyses reveal specific distribution of anti-bacterial molecule Perforin-2 in
385 human skin and its modulation by wounding and *Staphylococcus aureus* infection.
386 *Exp Dermatol.* 2019 Mar;28(3):225-232.
387
388 Svensson-Arvelund J, Ernerudh J. The Role of Macrophages in Promoting and Maintaining
389 Homeostasis at the Fetal-Maternal Interface. *Am J Reprod Immunol.* 2015 Aug;74(2):100-9
390
391 Wang WJ, Hao CF, Lin QD.
392 Dysregulation of macrophage activation by decidual regulatory T cells in unexplained recurrent
393 miscarriage patients. *J Reprod Immunol.* 2011 Dec;92(1-2):97-102.
394
395 Wang XQ, Zhou WJ, Hou XX, Fu Q, Li DJ. Trophoblast-
396 derived CXCL16 induces M2 macrophage polarization that in turn inactivates NK cells at the
397 maternal-fetal interface. *Cell Mol Immunol.* 2018 Dec;15(12):1038-1046
398
399 Xu Y, Romero R, Miller D, Kadam L, Mial TN, Plazyo O, Garcia-Flores V, Hassan SS, Xu Z,
400 Tarca AL, Drewlo S, Gomez-Lopez N. An M1-
401 like Macrophage Polarization in Decidual Tissue during Spontaneous Preterm Labor That Is
402 Attenuated by Rosiglitazone Treatment. *J Immunol.* 2016 Mar 15;196(6):2476-2491.
403
404 Zeldovich VB, Bakardjiev AI. Host defense and tolerance: unique challenges in the placenta.
405 *PLoS Pathog.* 2012;8(8):e1002804
406
407 Zhang YH, He M, Wang Y, Liao AH. Modulators of
408 the Balance between M1 and M2 Macrophages during Pregnancy. *Front Immunol.* 2017 Feb
409 9;8:120

410 *Figure Legends:*

411 **Fig. 1. Perforin-2 limits *L. monocytogenes* infection of the placenta and fetus.** Pregnant
412 *Perforin-2 (P2) +/+* and *-/-* mice were infected intravenously on GD 12.5 with 2.5×10^5 CFU of
413 *L. monocytogenes* for 44 hours. Bacterial loads were then determined in each individual liver,
414 placenta, and fetus by CFU assay. Shown are the compiled results of two separate infection
415 experiments using a total of 3 pregnant mice per genotype harboring a total of either 22 FPU_s (*P2*
416 *+/+*) or 17 FPU_s (*P2 -/-*). Mann-Whitney U test used to calculate p-values.

417

418 **Fig. 2: Both maternal- and fetal-encoded Perforin-2 contribute to protection of the placenta**
419 **and fetus.** A heterogenic mating strategy was used to generate pregnant mice that possessed
420 fetuses that were either *Perforin-2 (P2) +/-* or *-/-*. Pregnant mice (GD 12.5) were infected
421 intravenously with 2.5×10^5 CFU *L. monocytogenes* for 44 hrs. **(A)** A representative cross is
422 shown between a *P2 -/-* female and a *P2 +/-* male. Following infection, FPU_s (N=10) were
423 dissected, bacterial loads determined in each individual placenta and fetus by CFU assay, and
424 individual fetuses genotyped. In the example shown, fetuses #1-4 are *P2 +/-* and #5-10 are *P2 -/-*
425 . Asterisk denotes CFU values below detection limit. **(B)** Compiled analysis of crosses between
426 *P2 -/-* females, N=5 and *P2 +/-* males in which FPU_s lack maternal-derived P2, designated as
427 M(-/-). Placentas associated with *P2 +/-* fetuses (e.g., fetuses 1-4 in **(A)**) possess trophoblasts
428 T(+/-) with fetal-derived P2. Placentas associated with *P2 -/-* fetuses (e.g., fetuses 5-10 in **(A)**)
429 possess trophoblasts T(-/-) that lack fetal-derived P2. **(C)** Similar compiled analysis of crosses
430 between *P2 +/-* females, N=5 and *P2 -/-* males in which FPU_s possess maternal-derived P2,
431 designated as M(+/-). Placentas associated with *P2 +/-* fetuses possess trophoblasts, designated
432 as T(+/-), with fetal-derived P2. Placentas associated with *P2 -/-* fetuses possess trophoblasts,

433 designated as T(-/-), that lack fetal-derived P2. Compiled data drawn from three independent
434 infections performed on separate days. Mann-Whitney U test was used to calculate p-values. (NS
435 = not significant)

436

437 **Fig. 3: Composition of immune cells in liver and decidua of uninfected and infected GD12.5**
438 **pregnant mice.** Pregnant mice (GD 12.5) were either uninfected or intravenously infected with 1
439 $\times 10^6$ CFU of *L. monocytogenes* for 44 h. Single-cell preparations of the indicated tissue were
440 analyzed by flow cytometry for expression of immune- and myeloid-specific markers. **(A)** The
441 percentage of cells staining positive for the immune-specific cell surface marker CD45 per 10^6
442 isolated total live liver cells shown from an uninfected and infected mouse. The left panel shows
443 the staining profile of CD45-staining liver cells from an individual uninfected dam (top) and an
444 individual infected dam (bottom). The right panel shows the expression levels of myeloid-
445 specific markers CD11b and F4/80 of the CD45⁺ cells. **(B)** For the same mice, the percentage of
446 cells staining positive for the immune-specific cell surface marker CD45 per 10^6 isolated total
447 live decidual cells are shown. The left panel shows the staining profile of CD45-staining
448 decidual cells from an individual uninfected dam (top) and an individual infected dam (bottom)
449 and the right panel shows the expression levels of myeloid-specific markers CD11b and F4/80 of
450 the CD45⁺ cells. Shown is a representative mouse from 3 mice per group.

451

452 **Fig. 4: *Perforin-2* expression is induced in decidual and splenic immune cells following**
453 **infection** Pregnant BALB/c mice (GD12.5) were infected intravenously with 5×10^5 - 1×10^6 CFU
454 of *L. monocytogenes* for 44 hrs and decidual and splenic cells were analyzed for *P2* mRNA levels.

455 (A) Representative contour plots of background (FMO), uninfected, and infected cells gated on
456 live, CD45⁺ cells expressing AF-647 (P2). Histogram overlay of uninfected (red) and infected
457 (blue) CD45⁺ decidual cells showing *Perforin-2* (P2) mRNA levels. (B) Compiled analysis of P2
458 percentage and mean fluorescence intensity (MFI) of P2 expression on CD45⁺ cells in decida and
459 spleen. Compiled data drawn from two independent infections performed on separate days.
460 Student's T-test was used to calculate p-values.

461
462 **Fig. 5: Specific *Perforin-2* induction in decidual and splenic macrophages of BALB/c and**
463 **C57BL/6 dams following infection.** Pregnant BALB/c (A-C) and C57BL/6 (D-F) mice (GD12.5)
464 were infected intravenously with 5×10^5 - 1×10^6 CFU of *L. monocytogenes* for 44 hrs and decidual
465 and splenic macrophages were analyzed for *Perforin-2* (P2) mRNA levels. (A,D) Representative
466 contour plots of background (FMO), uninfected, and infected cells gated on live macrophages
467 expressing AF-647 (P2). Histogram overlay of uninfected (red) and infected (blue) CD45⁺ decidual
468 macrophages showing P2 mRNA levels. Compiled analysis of P2 percentage and mean
469 fluorescence intensity (MFI) of P2 expression in decidual macrophages (B,E) and spleen (C,F).
470 Compiled data drawn from two independent infections performed on separate days. Student's T-
471 test used to calculate p-values.

472
473 **Fig. 6: Divergent *Perforin-2* expression in decidual and splenic macrophages following lower-**
474 **dosed infections.** Pregnant BALB/c (A-C) or C57BL/6 (D,E) mice (GD 12.5) were infected
475 intravenously with 2.5×10^5 CFU of *L. monocytogenes* for 44 hrs and single-cell preparations of
476 decidual and splenic macrophages were analyzed for *Perforin-2* (P2) mRNA levels and shown as
477 described in Fig. 5. Student's T-test used to calculate significance. (NS = not significant)

478

479 **Fig. 7: Decidual macrophages polarize to a M1 phenotype following high-dose infection.**

480 Pregnant mice (GD 12.5) were either uninfected or intravenously infected with 1×10^6 CFU
481 (PD₁₀₀) of *L. monocytogenes* for 44 h. Single-cell preparations of deciduas were analyzed by flow
482 cytometry for expression of M1 and M2 macrophage-specific markers. **(A)** Gating strategy used
483 to define macrophages (single, live, CD45⁺, CD11b⁺, F4/80⁺, Ly6C⁻, Ly6G⁻). Gating strategy and
484 proportions of M2 (CD206⁺, MHCII^{lo}) and M1 (CD206⁻, MHCII^{hi}) macrophages in a
485 representative uninfected **(B)** and PD₁₀₀ infected **(C)** dam (GD 12.5). **(D)** Compiled analysis of
486 M1 and M2 decidual macrophages by percentage in uninfected and PD₁₀₀ infected dams. Results
487 based on 4 mice analyzed on several different days. Student's T-test was used to calculate p-values.
488

489 **Fig. 8: *Perforin-2* is expressed preferentially in decidual M1 macrophages.** Decidual cells
490 were isolated from uninfected pregnant *Perforin-2* (*P2*) ^{+/+} BALB/c mice (GD 12.5) and M1
491 and M2 macrophages were analyzed for *P2* mRNA. **(A)** Representative contour plots are shown
492 of background (FMO) and uninfected M1 (top) and M2 (bottom) macrophages expressing AF-
493 647 (*P2*). Histogram overlay plots of individual dams showing *P2* mRNA levels in M1 (clear)
494 and M2 (grey filled) decidual macrophages. **(B)** Compiled analysis of *P2* mRNA levels in M1
495 and M2 macrophages by percentage and mean fluorescence intensity (MFI) in decidua. Results
496 based on 5 uninfected dams. Student's T-test used to calculate p-values.

Fig. 1

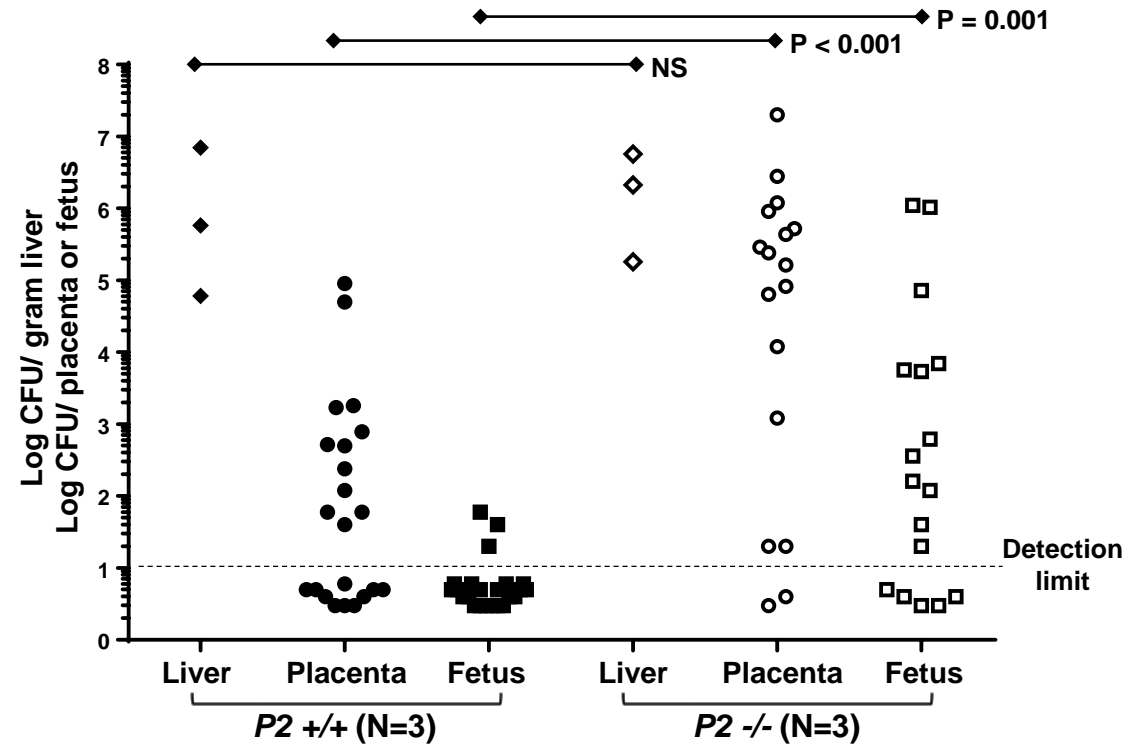


Fig. 2

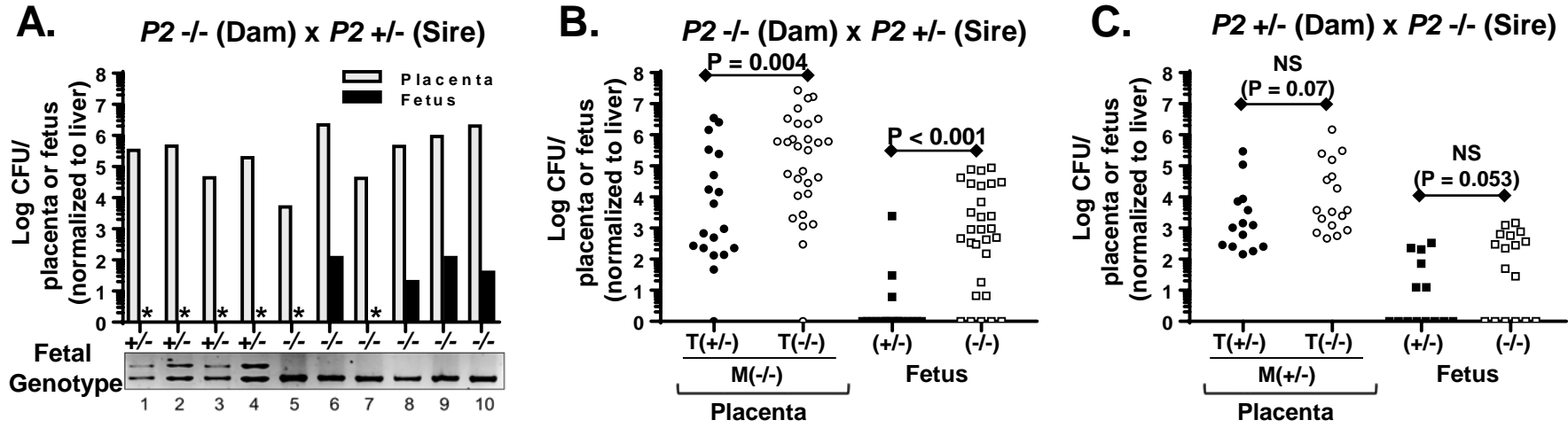


Fig. 3

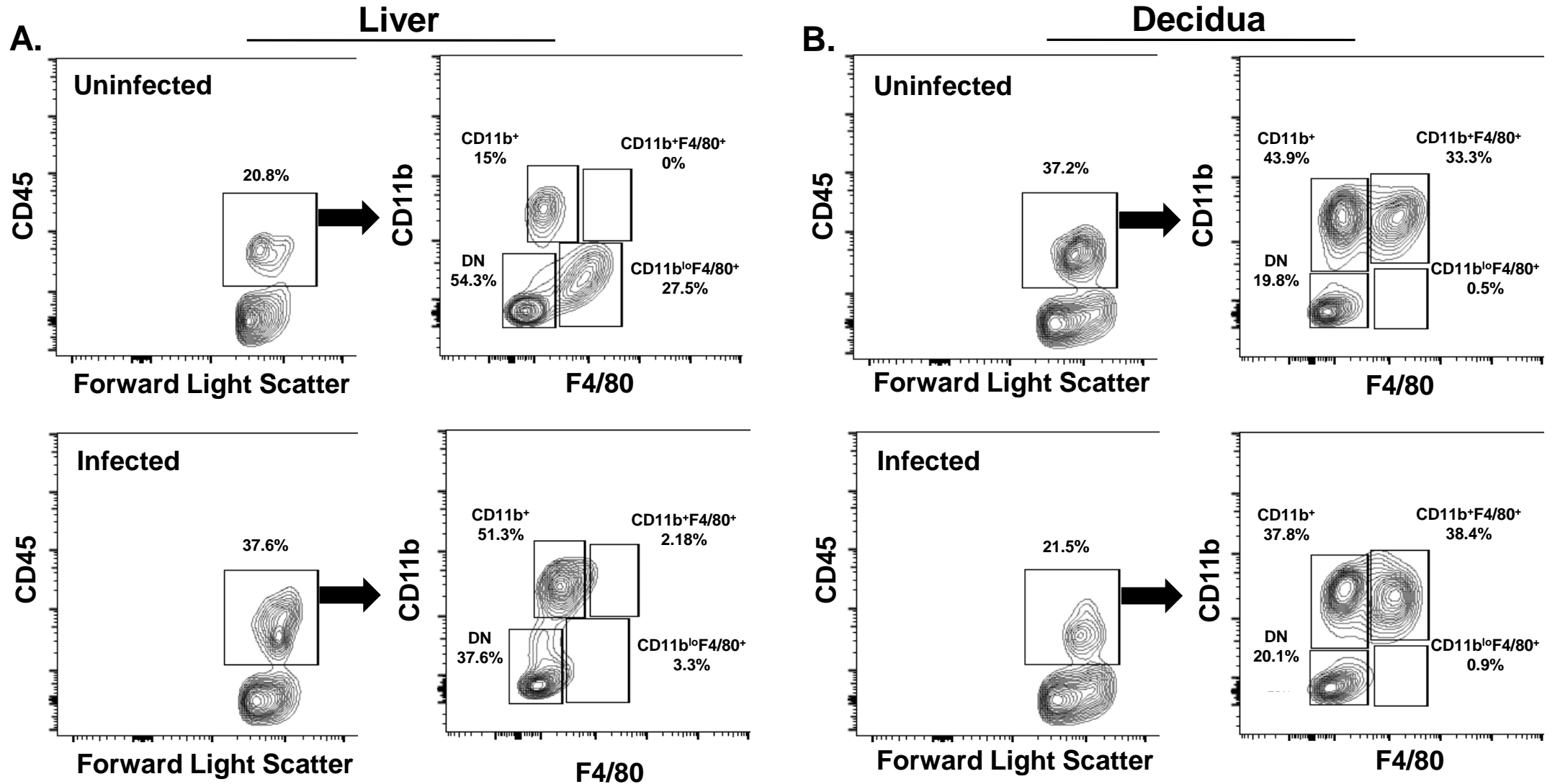


Fig. 4

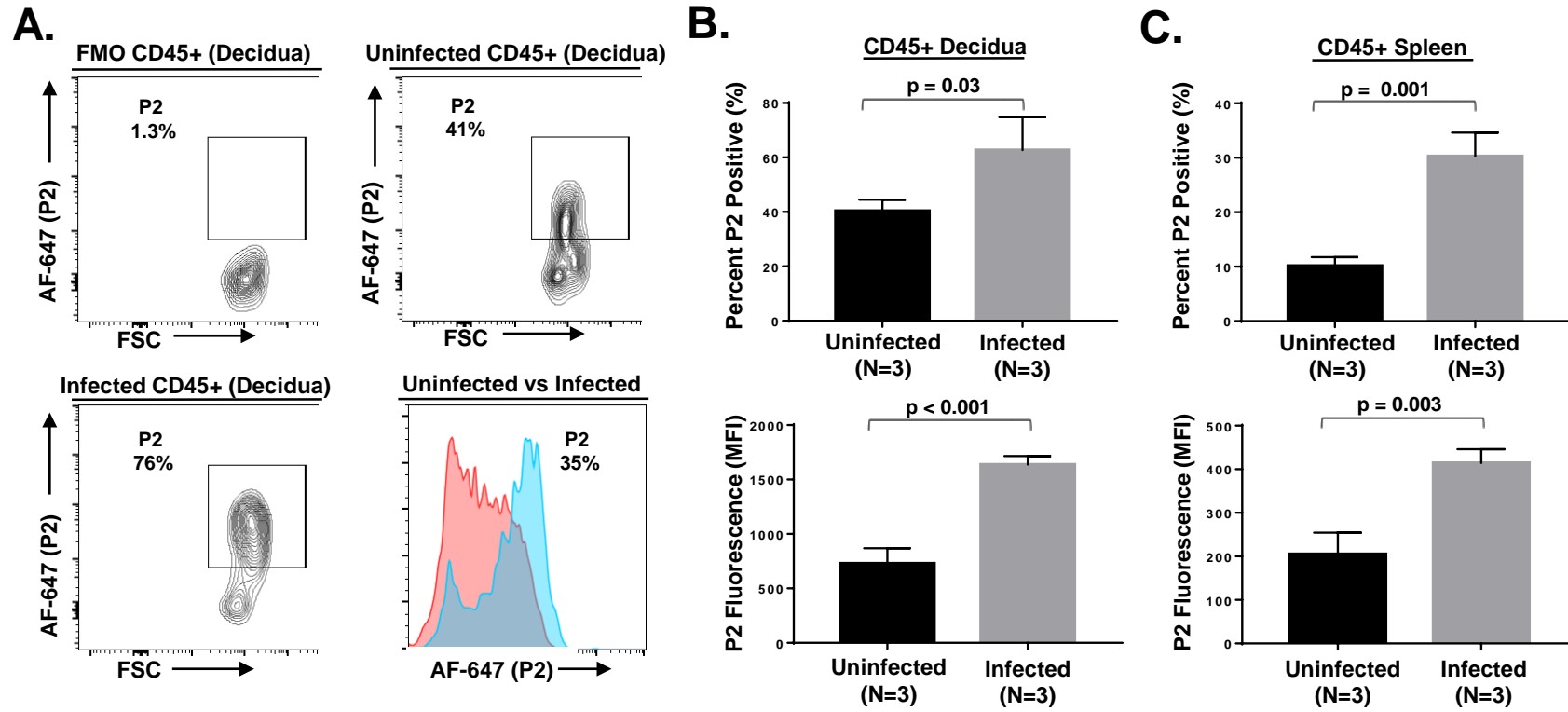


Fig. 5A,B,C

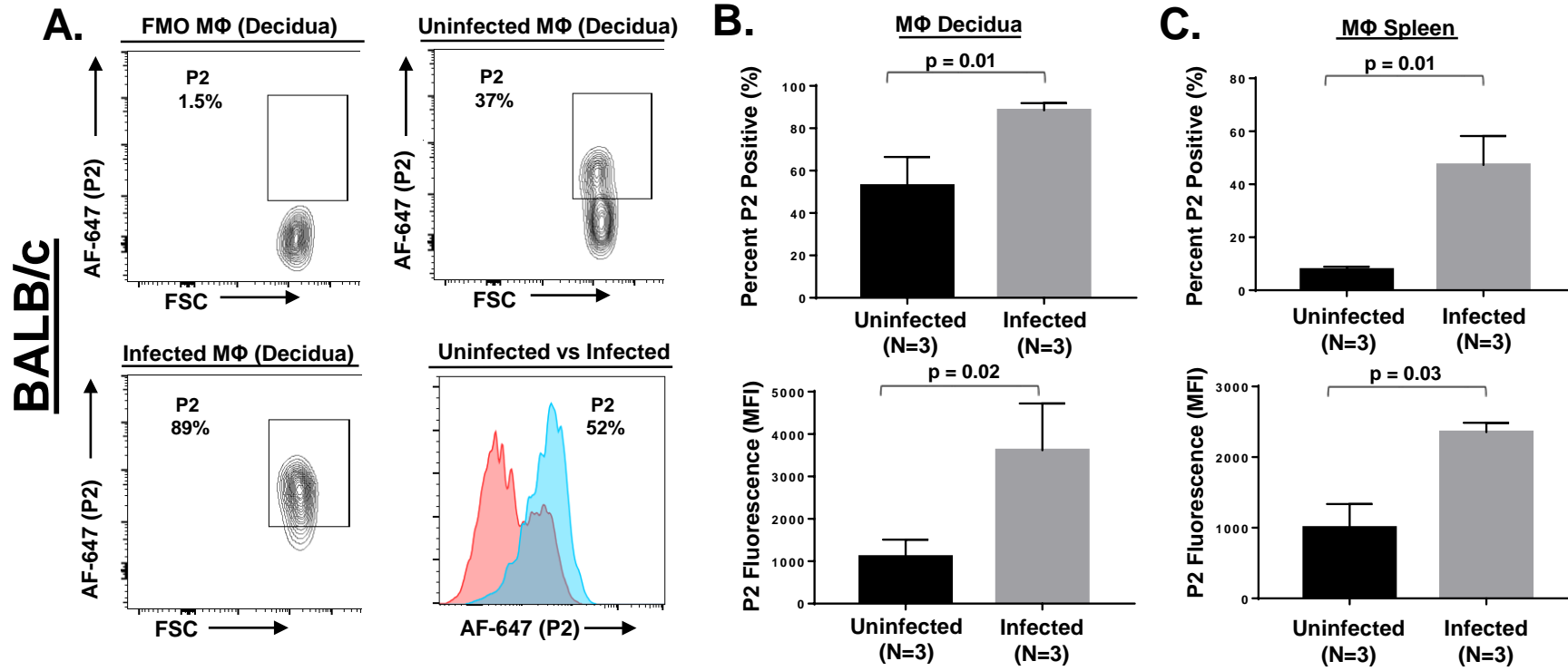


Fig. 5D,E,F

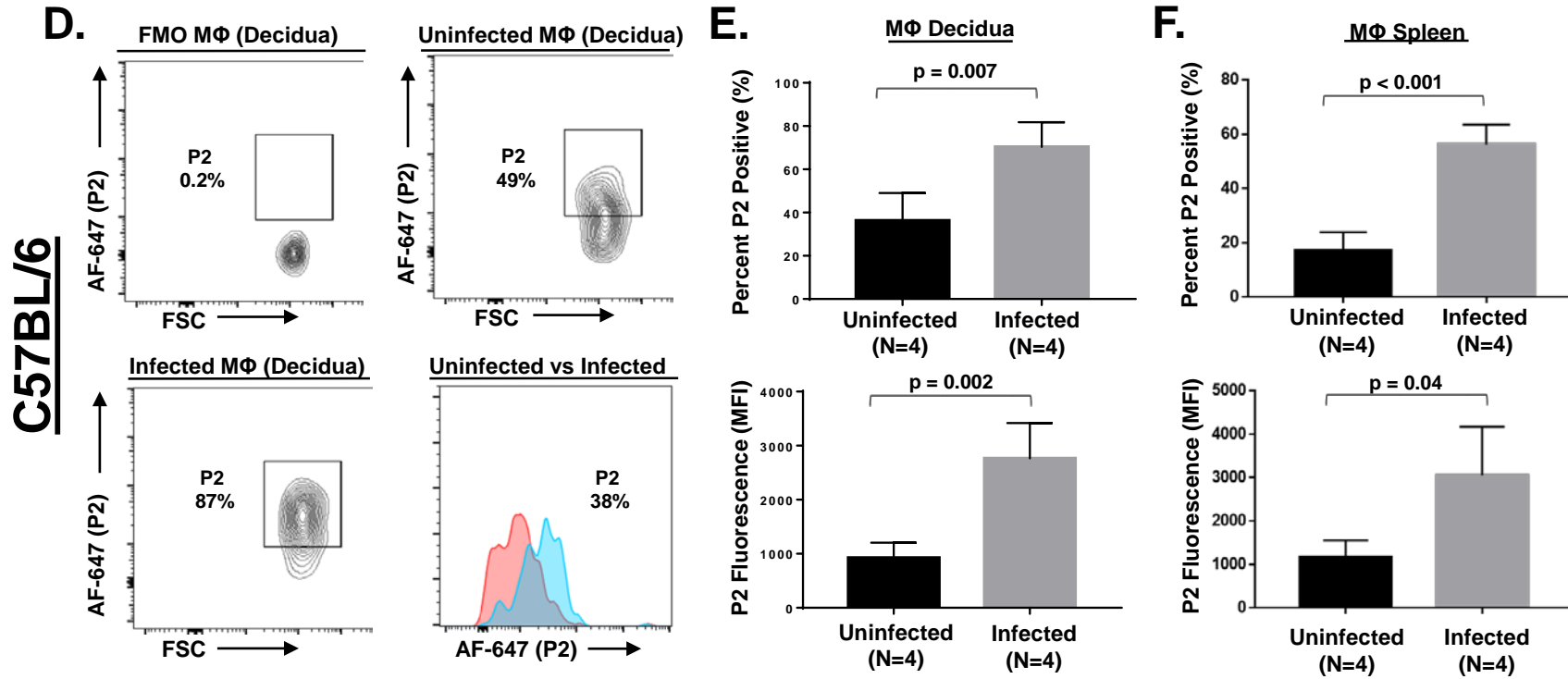


Fig. 6

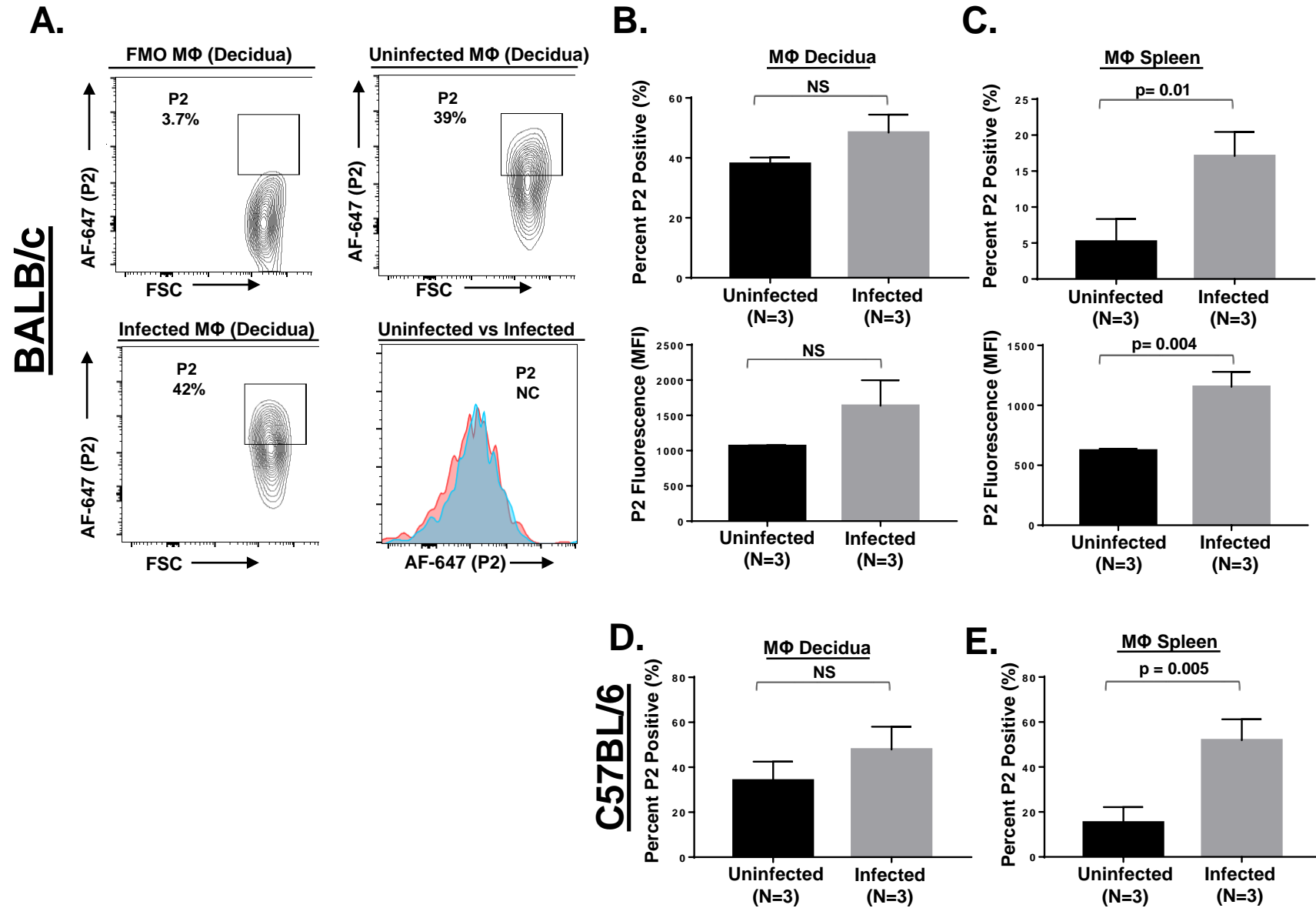


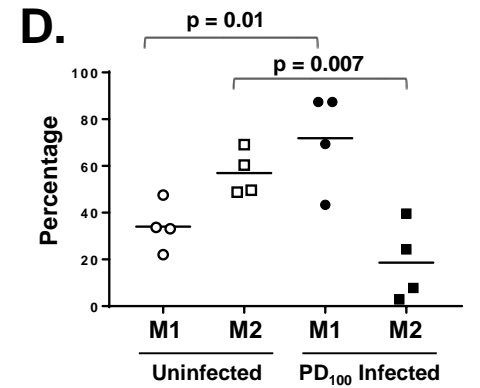
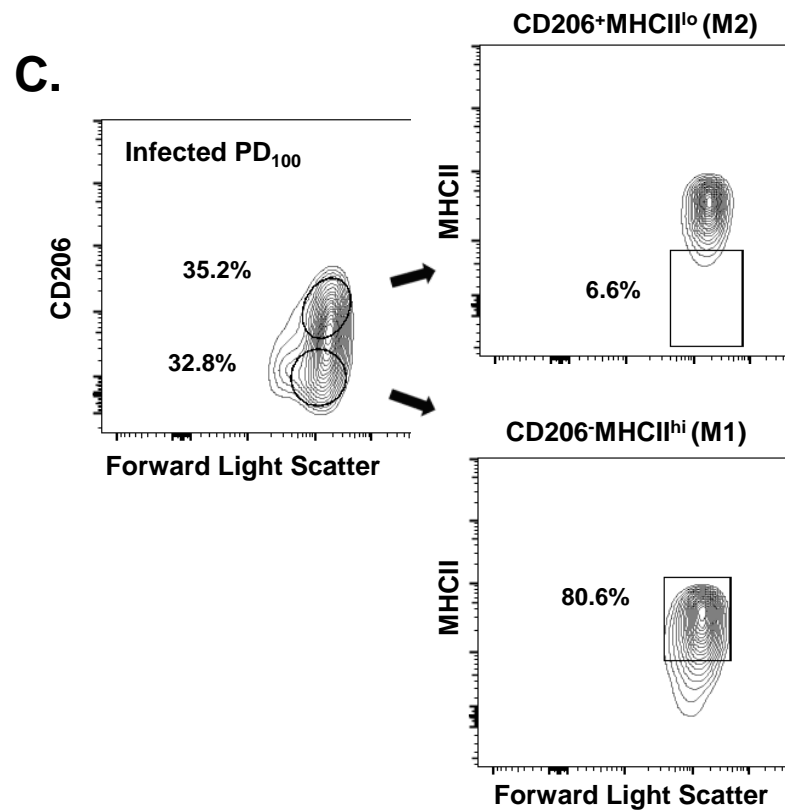
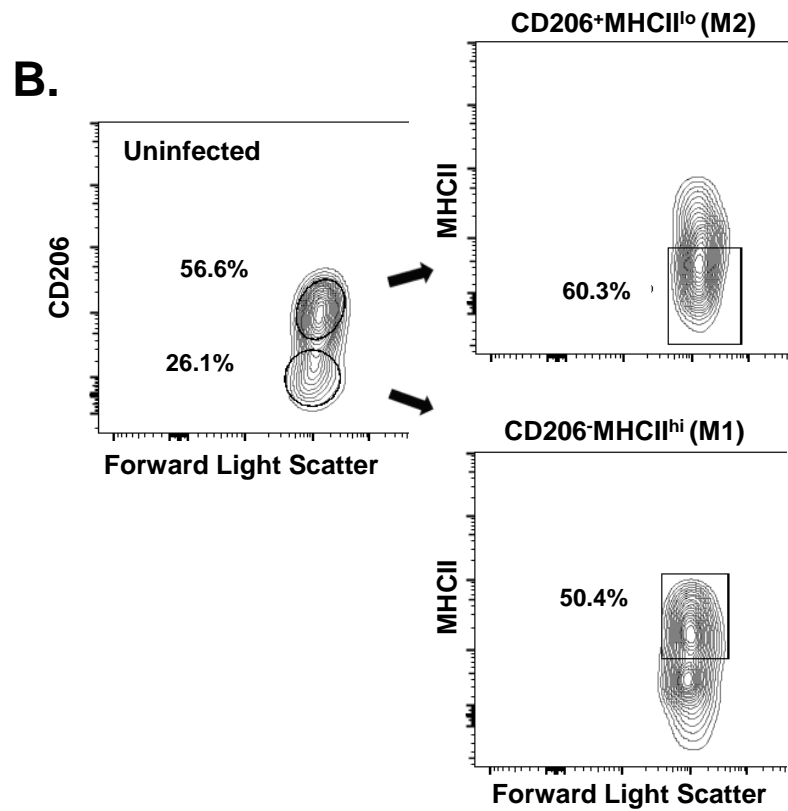
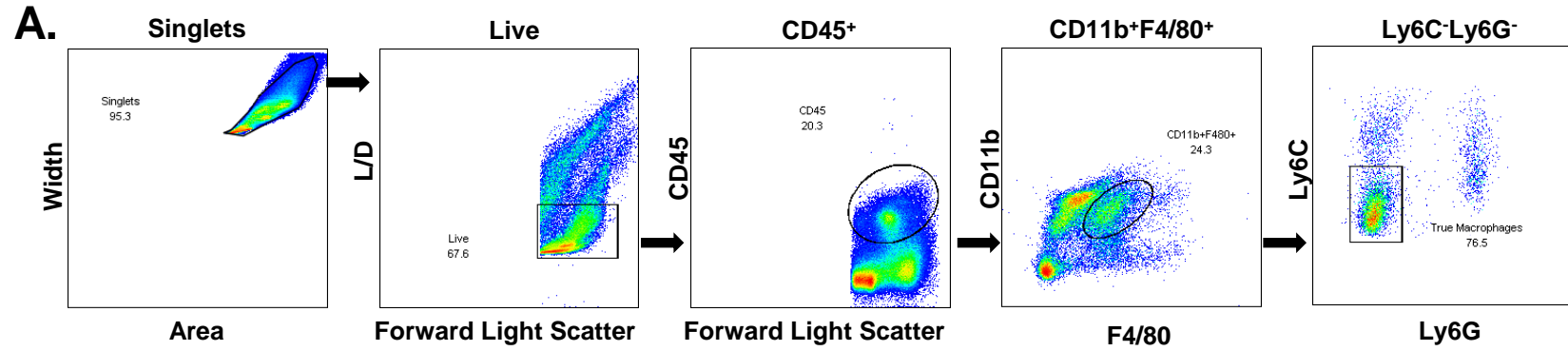
Fig. 7

Fig. 8

